



Highly sensitive electrochemical sensor based on carbon paste electrode modified with graphene nanoribbon–CoFe₂O₄@NiO and ionic liquid for azithromycin antibiotic monitoring in biological and pharmaceutical samples

Reza Mostafazadeh^{1,2} · Hassan Karimi-Maleh³ · Ali Ghaffarinejad^{1,4} · Fariba Tajabadi² · Yasamin Hamidian⁵

Received: 23 October 2022 / Accepted: 13 January 2023 / Published online: 24 January 2023
© King Abdulaziz City for Science and Technology 2023

Abstract

In this report, Azithromycin (Azi) antibiotic was measured by carbon paste electrode (CPE) improved by graphene nanoribbon–CoFe₂O₄@NiO nanocomposite and 1-hexyl-3 methylimidazolium hexafluorophosphate (HMIM PF₆) as an ionic liquid binder. The electrochemical behavior of Azi on the graphene nanoribbon–CoFe₂O₄@NiO/HMIM PF₆/CPE is investigated by voltammetric methods, and the results showed that the modifiers improve the conductivity and electrochemical activity of the CPE. According to obtained data, the electrochemical behavior of Azi is related to pH. Under optimum conditions, the sensor has linear ranges from 10 μM to 2 mM with a LOD of 0.66 μM. The effect of scan rate and chronoamperometry were studied, which showed that the Azi electro-oxidation is diffusion controlled with the diffusion coefficient of 9.22×10^{-6} cm²/s. The reproducibility (3.15%), repeatability (2.5%), selectivity, and stability (for 30 days) tests were investigated, which results were acceptable. The actual sample analysis confirmed that the proposed sensor is an appropriate electrochemical tool for Azi determination in urine and Azi capsule.

Keywords Macrolide antibiotic sensor · Azithromycin determination · 1-Hexyl-3 methylimidazolium hexafluorophosphate ionic liquid · Nanocomposite · Voltammetry

Introduction

Azithromycin (Azi) is a potent macrolide antibiotic that is one of the most effective antibiotics for treating severe infections (Nigović 2004). Azi has treated some acute bacterial infections, such as lung, ear, and skin infections (Parnham et al. 2014). Bacteria need a unique process of protein synthesis activated by ribosomal proteins to multiply. Azi inhibits bacterial protein synthesis by inhibiting the transpeptidation/translocation phase and by inhibiting 5 s ribosomal subunit assembly, which leads to the control of various bacterial infections (Champney and Burdine 1995). The global outbreak of COVID-19 has prompted researchers to try to find drugs to treat the disease. Azi, in combination with hydroxychloroquine or chloroquine, has been suggested as one of these drugs (Sultana et al. 2020). The combination of this drug with hydroxychloroquine can treat acute respiratory syndromes (Gautret et al. 2021). Furthermore, the unusual interaction between Azi and simvastatin is the cause of rhabdomyolysis (Alreja et al. 2012). On the

✉ Ali Ghaffarinejad
Ghaffarinejad@iust.ac.ir

- ¹ Research Laboratory of Real Samples Analysis, Faculty of Chemistry, Iran University of Science and Technology (IUST), Tehran 1684613114, Iran
- ² Department of Nanotechnology and Advanced Materials, Materials and Energy Research Center, PO Box 31787-316, Karaj, Iran
- ³ School of Resources and Environment, University of Electronic Science and Technology of China, Xiyuan Ave, P.O. Box 611731, Chengdu, People's Republic of China
- ⁴ Electroanalytical Chemistry Research Center, Iran University of Science and Technology (IUST), Tehran 1684613114, Iran
- ⁵ Department of Chemistry, K. N. Toosi University of Technology, Tehran 16315-1618, Iran

other hand, environmental pollution caused by antibiotic drugs, especially Azi has been known as one of the most critical environmental issues (Baladi et al. 2022; Torkian et al. 2022). So, Azi determination in biological, pharmaceutical, and water samples is an essential subject. A variety of techniques, such as microbiological (Breier et al. 2002), spectroscopy (Jayanna et al. 2012; Rachidi et al. 2006), liquid chromatography (Choemunng and Na-Bangchang 2010; Filist et al. 2014), and high-performance liquid chromatography (Shepard et al. 1991; Zeng et al. 2014) have been reported for Azi determination. Despite sensitivity and accuracy, these methods require expensive equipment, long analysis times, hazardous solvent, and sophisticated sample preparation methods (Buledi et al. 2022). On the other hand, the electrochemical sensors are simple, eco-friendly, and low-cost, with short analysis time and acceptable sensitivity, selectivity, and accuracy (Heidari and Ghaffarnejad 2019; Bijad et al. 2021; Karimi-Maleh et al. 2022a, b; Rao et al. 2022). Hence, the electrochemical methods have been employed in several applications for instance analysis of ingredients in food products to evaluate food quality as a critical issue, as well as, electrochemical sensors have had a significant role in water pollution investigation as a highlighted issue, and for the determination of the drugs (Bijad et al. 2021; Karimi-Maleh et al. 2010, 2022c; d; Ensafi et al. 2011a, b; Karimi-Maleh 2013; Ensafi and Karimi-Maleh 2010; Zheng et al. 2022; Hojjati-Najafabadi et al. 2022a, b; Abedini et al. 2022; Ghaffarnejad et al. 2014; Karimi et al. 2022). In electrochemical determinations usually, the bare electrode has some limitations, such as poor electroactive sites, high resistance of electron transfer, and low sensitivity. Bare electrodes modification with nanomaterials is one of the common ways for overcoming these limitations (Karimi-Maleh et al. 2022b; Ashrafzadeh Afshar et al. 2022; Karaman et al. 2022; Jafarzadeh et al. 2022). Due to specific and significant properties that have been provided by nanomaterials, these materials have been noted and widely used in various fields of science and technology, such as energy storage, environmental application, sensor, food safety, hydrogen production, catalyst, biotechnology, optics, and electronics (Buledi et al. 2022; Karimi-Maleh et al. 2022c; Hojjati-Najafabadi et al. 2021, 2022a; c; Ashrafzadeh Afshar et al. 2022; Karaman et al. 2022; Jafarzadeh et al. 2022; Khatoun et al. 2022; Coguplugil 2022; Hashemi et al. 2022; Mansoorianfar et al. 2022).

Several studies have reported the application of electrochemical techniques to determine Azi, using various electrode surface modification protocols that increase sensor sensitivity (Zhou et al. 2016; Hu et al. 2018; Vajdle et al. 2020; Farghaly and Mohamed 2004; Ensafi et al. 2013). In this work, we introduce an electrochemical sensor based on a carbon paste electrode amplified by nanoribbon-CoFe₂O₄@NiO nanocomposite and HMIM PF₆

ionic liquid for sensitive, selective, and wide linear range determination of Azi in various real samples.

Experimental

Materials and reagents

The graphite powder (spectroscopic grade, particle size < 50 μm) was used as the main structure of the electrode, and ortho-phosphoric acid (85%), H₂SO₄ (98%), paraffin oil (*d* = 0.86 kg/l), NaOH, KMNO₄ (> 99%) and 1-hexyl-3 methylimidazolium hexafluorophosphate (> 97%) supplied by Merck. Moreover, -COOH functionalized multiwalled carbon nanotubes (MWCNT, > 97%) were acquired from the US. Research Nanomaterials, Inc. Azithromycin (> 98%) (C₃₈H₇₂N₂O₁₂), CoCl₂·6H₂O (98%), FeCl₃ (97%), Ni (NO₃)₂·6H₂O (> 97%) and hydrogen peroxide purchased from Sigma-Aldrich company. Also, the co-precipitation method is used to prepare CoFe₂O₄ nanoparticles (Maaz et al. 2007). Chemicals are used without purification, and the aqueous solutions are prepared with deionized water.

Instrumentation

In this study, the electrochemical investigation was done by the potentiostat/galvanostat model of μ-Autolab Type II. so that, Ag/AgCl/3 M KCl used as a reference electrode, Pt wire, and Graphene nanoribbon-CoFe₂O₄@NiO/HMIM PF₆/CPE used as counter and working electrodes in the electrochemical cell. The electrochemical data were processed with Nova 1.11 software. The morphology studies were performed by the field emission scanning electron microscope (FESEM-MIRA3TESCAN-XMU). Moreover, XRD patterns were obtained in 2θ between 0° and 80° (0.02θ/s) with a Philips-PW 1800 diffractometer, which was equipped with Cu-Kα irradiation (λ = 0.1524 nm) source.

Synthesis of CoFe₂O₄@NiO

To synthesize CoFe₂O₄@NiO, 2.99 g Ni (NO₃)₂·6H₂O and 0.8 g sodium hydroxide were put in separate containers. Then added, 20 mL DI water to each container. Then 0.2 g CoFe₂O₄ was added into the nickel nitrate solution and dispersed, and NaOH dropwise addition was done via a burette. The mixture was filtered using filter paper after 90 min stirring. The precipitate was dried at 80 °C for 20 h in the oven after washing it with DI water. Finally, the calcination was done at 300 °C for 2 h (Mahmoudi and Behnajady 2018).

Synthesis of graphene nanoribbon–CoFe₂O₄@NiO nanocomposite

The graphene nanoribbon synthesized in our previous research method was mixed with CoFe₂O₄@NiO in a 4:1 weight ratio in the presence of 30 mL ethanol as solvent, then stirred for 2 h. In the next step, the dispersed solution was poured into an autoclave at 80 °C for 18 h. then, the autoclave content was centrifuged and washed with ethanol/DI water. Finally, the precipitate dried in the oven at 60 °C (Mostafazadeh et al. 2022).

Fabrication graphene nanoribbon–CoFe₂O₄@NiO/HMIM PF₆/CPE

Graphene nanoribbon–CoFe₂O₄@NiO/HMIM PF₆/CPE was prepared by mixing 0.94 g graphite powder and 0.06 g graphene nanoribbon–CoFe₂O₄@NiO in diethyl ether solvent. HMIM PF₆ and paraffin oil were added as binders with optimal value after diethyl ether evaporated. The fabricated paste was placed in a glass tube, and the electrical contact was performed with a copper wire and used as an electrochemical sensor (Abdi et al. 2020).

Real sample preparation

The fabricated sensor was evaluated by urine and azi capsules as real samples. The urine sample was centrifuged (3000 rpm) for 5 min and then filtered to obtain a solution without any solid particles. Then 7.5 mL of real sample was added with 7.5 mL of phosphate buffer solution (PBS) (pH 7.0, constant amount of 20% ethanol) in an electrochemical cell (Mater Mahnashi et al. 2021).

The contents of one Azi capsule containing 250 mg Azi was grounded and homogenized, which was transferred to a 200 mL beaker, and 10 mL of ethanol with 30 mL of DI water was added to the beaker. Then, the resulting mixture was sonicated for 5 min to the dissolution of Azi, then the undissolved portion was filtered. In the next step, the obtained solution was transferred to a 50 mL volumetric flask and used as a real sample by diluting it to the mark with DI water. Finally, 30 µL of the solution with 15 mL of the PBS was input into the electrochemical cell. The real sample analysis was done by using the standard addition method (Ensafi et al. 2013).

Results and discussion

Characterization of nanocomposite

The X-ray diffraction pattern of graphene nanoribbon–CoFe₂O₄@NiO nanocomposite was obtained to

characterize phase structure and crystalline nature. Figure 1 shows that the obtained graphene nanoribbon–CoFe₂O₄@NiO nanocomposite is mostly in the amorphous phase. Also, the pattern shows six diffraction peaks, one at $2\theta = 25^\circ$ (corresponding to the diffraction peaks of graphene nanoribbons), and others at 36.5, 57, 42.9 and 62° can be assigned to CoFe₂O₄ (Reference code 96-101-0096) and 37.2, 43, and 62° for NiO (Reference code 00-002-1216). Furthermore, the grains size was calculated by the Scherrer equation expressed below:

$$D = k\lambda / (\beta \cos\theta),$$

where D is the crystallite particle size (nm), the value of Scherrer constant (k) is equal to 0.89, λ is the X-ray wavelength, β is the width of the peak at half maximum intensity (FWHM), and θ is the diffraction angle (Scherrer 1912). According to the formula, the CoFe₂O₄@NiO size crystallite was 14.55 nm.

The morphological characteristics of graphene nanoribbon–CoFe₂O₄@NiO nanocomposite as a powder material for modifying the carbon paste electrode were investigated by scanning electron microscope (SEM). Figure 2a belonged to graphene nanoribbon before decorating by CoFe₂O₄@NiO, which was prepared as the suitable base for nanocomposite. then, the particles of CoFe₂O₄@NiO dwelled on the graphene nanoribbon, and the randomly distributed small to large aggregated particles of CoFe₂O₄@NiO on the graphene nanoribbon surface can be seen in Fig. 2b.

The energy-dispersive X-ray spectroscopy (EDS) spectra of graphene nanoribbon, CoFe₂O₄@NiO, and graphene nanoribbon–CoFe₂O₄@NiO discernibly authenticate the successful ornament of nanoparticles. No additional element as an impurity was detected in the EDX spectra that implicate the ultra-purity of the prepared material. Furthermore, Fig. 3b approves of the elemental

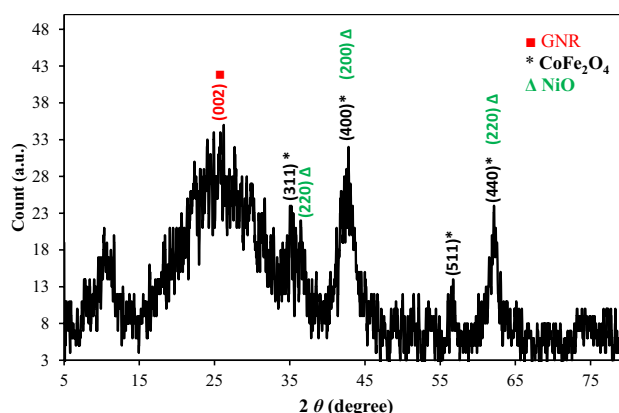


Fig. 1 XRD pattern of graphene nanoribbon–CoFe₂O₄@NiO composite

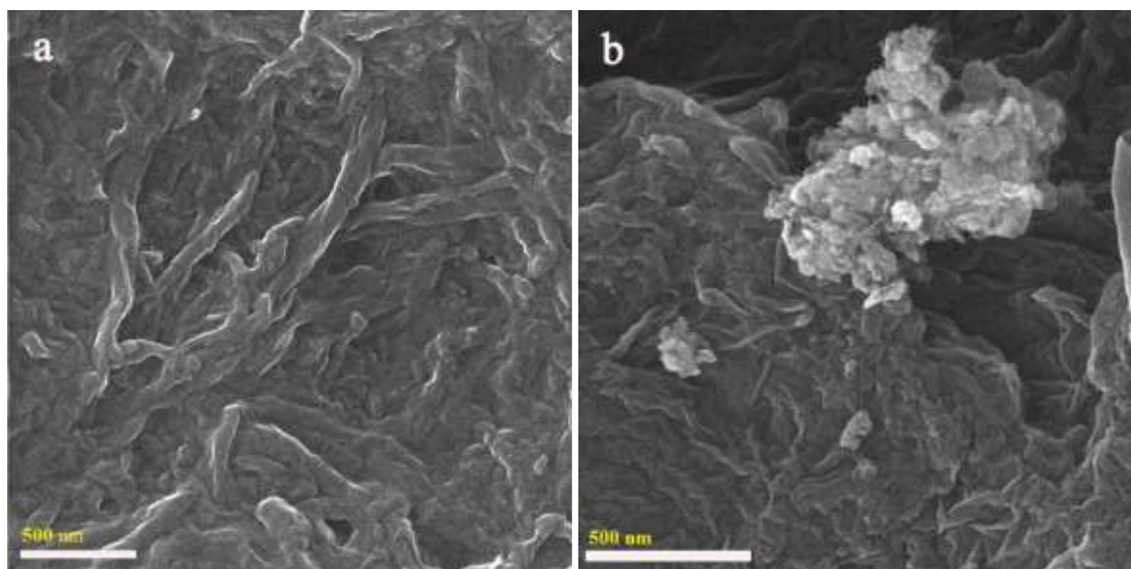


Fig. 2 Scanning electron microscopy (SEM) micrographs of **a** graphene nanoribbon, **b** graphene nanoribbon–CoFe₂O₄@NiO nanocomposite

existence of carbon, oxygen, iron, Cobalt, and nickel in the nanocomposite. Moreover, the EDS spectra confirmed that CoFe₂O₄@NiO particles illustrate good affinity to graphene nanoribbon matrix without any impurity (Fig. 3a, b).

Electrochemical characterization of Azithromycin at different modified CPE electrodes

In this report, the carbon paste electrode was amplified by graphene nanoribbon–CoFe₂O₄@NiO and HMIM PF₆. The effect of this modification was investigated by recording square wave voltammetry (SWV) in the potential range of 0.65–1.2 V with a potential amplitude of 20 mV and frequency of 10 Hz at bare CPE, graphene nanoribbon–CoFe₂O₄@NiO/CPE, (HMIM PF₆)/CPE and graphene nanoribbon–CoFe₂O₄@NiO/HMIM PF₆/CPE in 500 μM of Azi. According to Fig. 4, square wave voltammograms, oxidation currents increase from 3.5 μA on bare CPE to 4.03, 8.2, and 10.41 μA on different modified CPE. So, by moving curve A toward curve D, the lowest oxidation current related to the bare carbon paste electrode, which is due to weak redox activity in detecting Azi, and the highest oxidation peak belongs to graphene nanoribbon–CoFe₂O₄@NiO/HMIM PF₆/CPE due to the high availability of electroactive sites that were created by increasing the surface area. Higher surface area and presence of ionic liquid led to a decrease in electrode resistance and an increase in the charge transfer process.

Investigation of concentration, scan rate, and pH effects

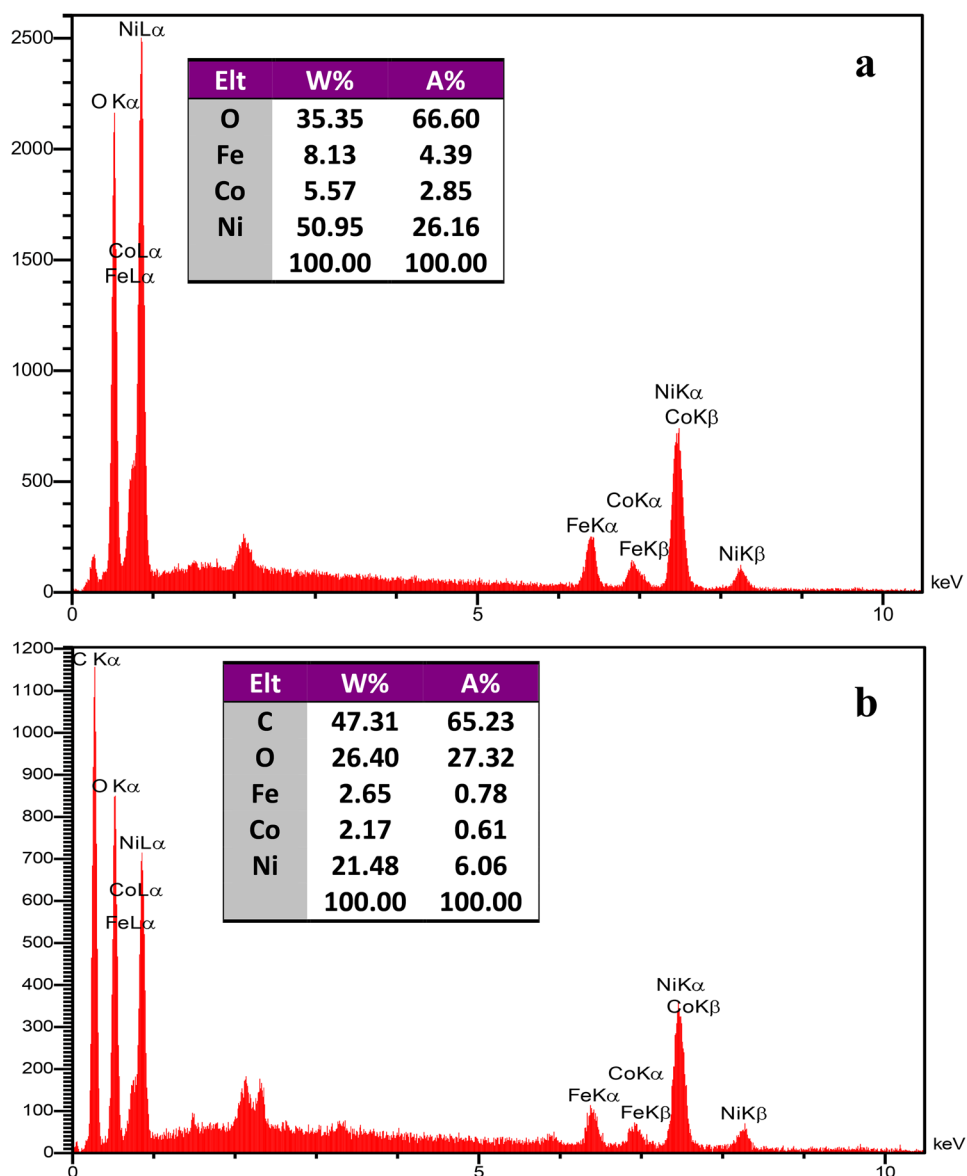
The performance of the Azi sensor was evaluated by SWV in different concentrations of Azi solution, which achieved the linear relationship from 60 μM to 1 mM as shown in Fig. 5.

The scan rate effects were investigated, and the results are shown in Fig. 6. In this study, several cyclic voltammograms with different scan rates from 10 to 250 mV/s were applied in 500 μM Azi solution. As Fig. 6 shows, the linear relationship ($R^2=0.9954$) between anodic peak current and $U^{1/2}$, which reveals a diffusion-controlled process for electro-oxidation of Azi at the surface of graphene nanoribbon–CoFe₂O₄@NiO/HMIM PF₆/CPE (Abdi et al. 2020; Motaghi et al. 2016; Jahani et al. 2020; Bijad et al. 2018; Shamsadin-Azad et al. 2019; Tajik et al. 2014).

To calculate diffusion coefficient value (D), the chronoamperometry study was done at graphene nanoribbon–CoFe₂O₄@NiO/HMIM PF₆/CPE in 100, 200, 300, and 400 μM of Azi at potential 1100 mV. Moreover, Cottrell's plot ($I-t^{-1/2}$) for Azi at the suggested electrode is obtained and depicted in Fig. 7 (inset). According to this study, the value of D was equal to 9.22×10^{-6} cm²/s.

For investigation of the pH effect, voltammograms of Azi solution were recorded at graphene nanoribbon–CoFe₂O₄@NiO/HMIM PF₆/CPE in different pH values (5–9) (Fig. 8a inset). According to data from Fig. 8, oxidation potential is decreased by increasing pH, which shows the participation of proton in the oxidation mechanism process of Azi as reported previously (Shawabkeh and Tutunji 2002). Also,

Fig. 3 EDS spectra of **a** CoFe₂O₄@NiO and **b** graphene nanoribbon–CoFe₂O₄@NiO



the highest peak current was observed at pH 7.0, which was the optimum pH for electrochemical analysis (Fig. 8b). On the other hand, the result showed a negative slope between Azi oxidation potential signal vs. pH with equation $E_{pa} = -0.0565 \text{ pH} + 1.2919$ ($R^2 = 0.9908$). The Nernstian slope shows that the number of protons and electrons in the oxidation reaction is equal.

Azithromycin oxidation behavior

The reaction mechanism of Azi is verified by studying pH, and scan rate. The methyl groups determine Azi hydrophobicity by ionizable agents covering. Azi is protonated at pH 7.0 at both N₃ and N₉ and is a highly hydrophobic molecule (Sharma and Hwa 2022). Azi tends to diffuse at

the surface. herein, the oxidation half-reaction is facilitated by highly electroactive sites, which are formed by CoFe₂O₄@NiO and ion liquid. The amine groups in the structure of azithromycin are most easily oxidized. So, the alkylamine change to radical cation form by losing an electron (Grimshaw 2000). The obtained anodic peak current is related to electrons of N₃ because N₉ does not lose lone pair of electrons easily due to its location in the macrocyclic lactone ring. The similar electrochemical responses of erythromycin as a structural analogous drug with no nitrogen in the macrocyclic lactone ring are approved of N₃ participation in the electrochemical mechanism of Azi (Gielen et al. 2010; Chorin et al. 2020; Wang et al. 2000; Montenez et al. 1996; Peng et al. 2011; Mandić et al. 2003). The electrochemical mechanism is shown in Scheme 1.

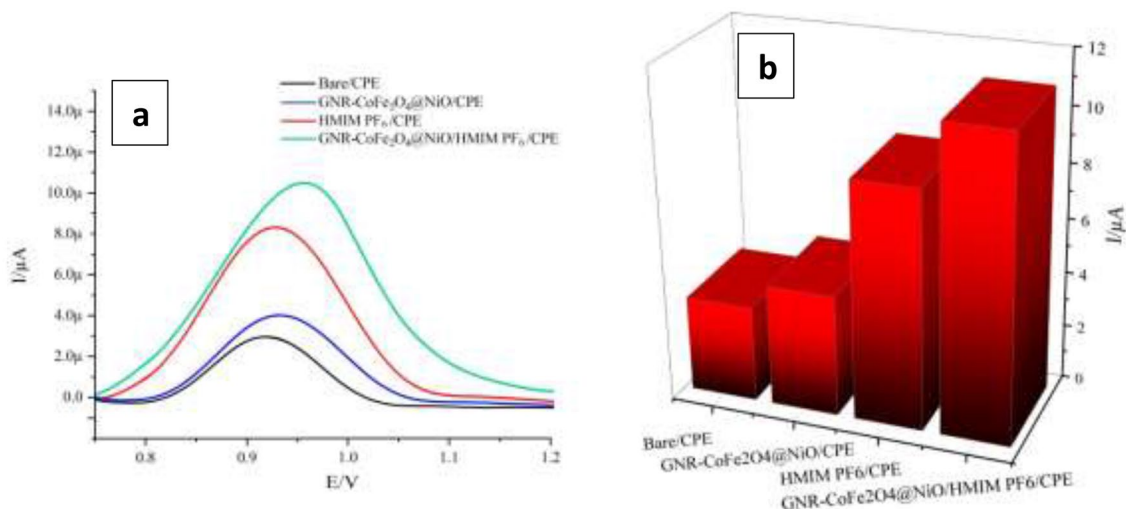


Fig. 4 **a** Square wave voltammograms of 500 μM Azi at CPE, graphene nanoribbon–CoFe₂O₄@NiO/CPE, (HMIM PF₆)/CPE, and graphene nanoribbon–CoFe₂O₄@NiO/HMIM PF₆/CPE. **b** Current response to different modified electrode

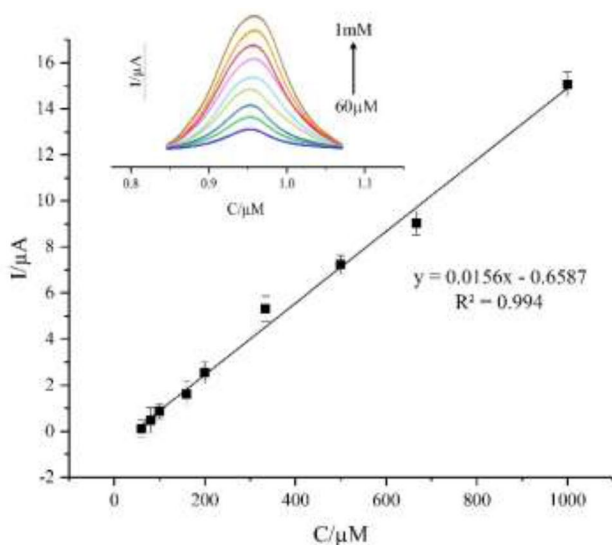


Fig. 5 Calibration curve obtained at different concentrations of the Azi on graphene nanoribbon–CoFe₂O₄@NiO/HMIM PF₆/CPE in PBS (pH 7.0, $n = 3$). Inset is the SWVs obtained from different concentrations of Azi

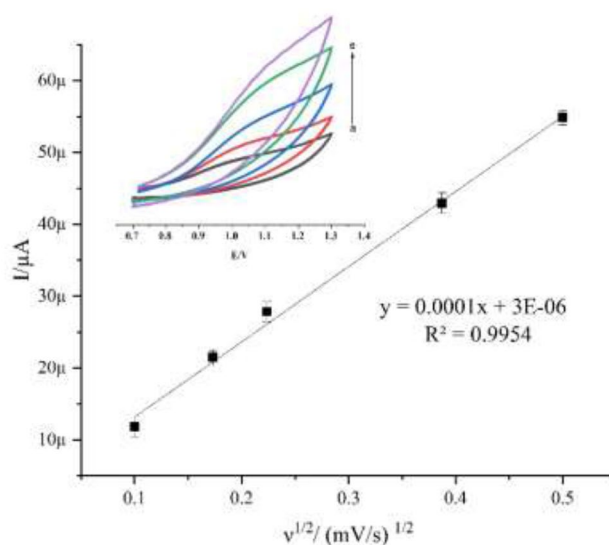


Fig. 6 The plot of $I_{pa}/v^{1/2}$ for oxidation of 500 μM Azi at the suggested sensor ($n = 3$). Inset: cyclic voltammograms 500 μM Azi at different scan rates from 10 to 250 mV/s

The linear dynamic range and limit of detection

Square wave voltammetry was used as a sensitive technique for investigating the linear dynamic range of Azi concentration (Fig. 9 inset). The investigation was done in the concentration range of 10 μM–5 mM. According to the results shown in Fig. 9, the oxidation peak current (I_{pa}) is improved by increasing the concentration from 10 μM to 2 mM. Also, a linear relationship with equation

$I_{pa} = 0.011x + 0.3443$ ($R^2 = 0.9922$) was obtained in this range. Furthermore, a linear relation between 60 μM and 1 mM with the equation of $I_{pa} = 0.0156x - 0.6587$ and the correlation coefficient of $R^2 = 0.9940$ was observed. The calculated limit of detection (LOD) was equal to 0.66 μM ($S/N = 3$). The results show that a fabricated sensor is a suitable tool for determining Azi compared to previous reports (Table 1). In general, compared to most of the related reports in Table 1, the proposed sensor has a comparable or better figure of merits.

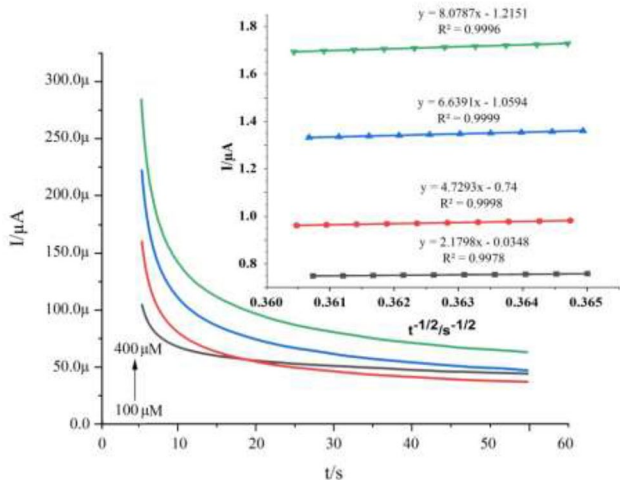


Fig. 7 Chronoamperograms of 100 to 400 μM of Azi at the suggested sensor. Inset: Cottrell's plot obtained from chronoamperograms

Stability, reproducibility, repeatability, and selectivity analysis

Stability as an essential factor for the fabricated sensor was obtained by square wave voltammetry method at graphene

nanoribbon–CoFe₂O₄@NiO/HMIM PF₆/CPE in the presence of 500 μM Azi solution. This evaluation was done for 30 days. The data obtained from the oxidation signals of Azi showed that the changes were less than 3.41% initial current which is an acceptable value for an electrochemical sensor. Moreover, we used five different electrodes with the same process preparation, and the response of the electrodes with the RSD value of 3.15% was obtained, which confirmed the acceptable reproducibility of the fabricated electrochemical sensor.

Moreover, the RSD to the repeatability of the sensor was recorded by five consecutive square wave voltammograms and calculated as 2.5%, which represents the admissible repeatability for the designed sensor. Alongside this, the selectivity of the engineered sensor has been verified in the presence of possible real sample interferences of an analyte such as metal cations, anions, and organic compounds. For this purpose, the fabricated electrochemical sensor was evaluated in 500 μM of Azi with mentioned interferences. According to data, 500-fold of Na⁺, K⁺, Br⁻, Cl⁻, 400-fold glucose, 300-fold of sucrose and urea, and 100-fold of thiamine have no interference for Azi determination at the surface of the fabricated sensor.

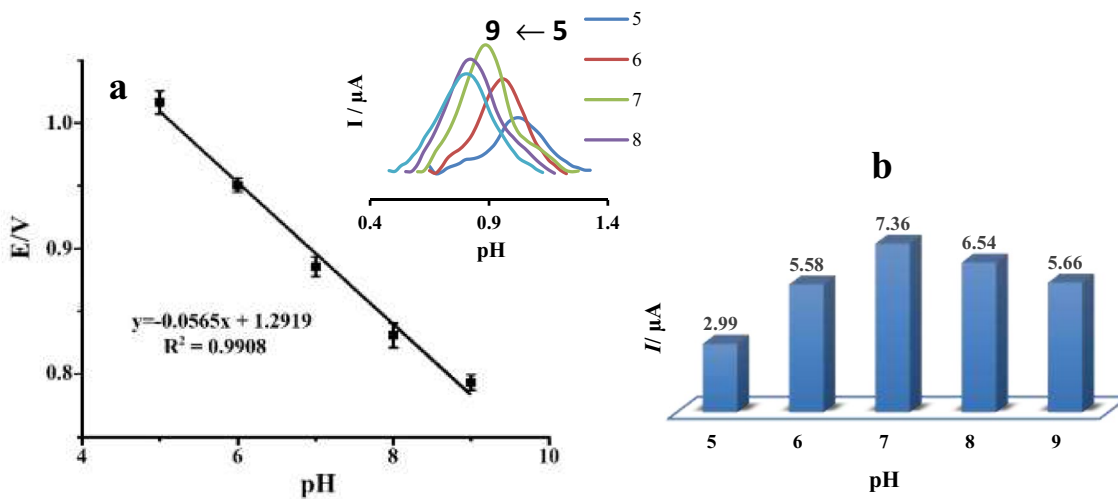
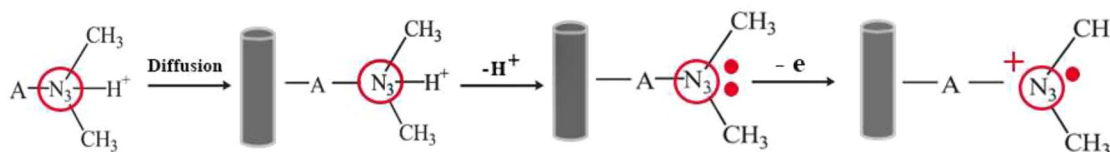


Fig. 8 **a** E–pH curve for electro-oxidation of 500 μM of Azi (*n* = 3). Inset: differential pulse voltammograms of 500 μM at graphene nanoribbon–CoFe₂O₄@NiO/HMIM PF₆/CPE. **b** Current responses of the suggested electrode in pH₅ ranging from 5 to 9



Scheme 1 Electrochemical mechanism of Azi towards the fabricated sensor

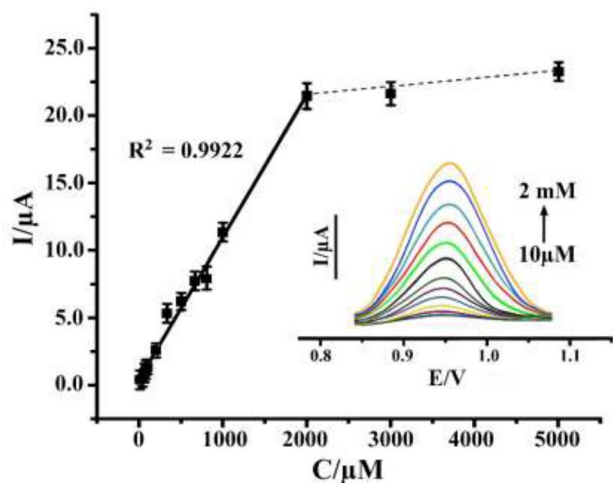


Fig. 9 The plot of I_{pa} vs. Concentration of Azi ($n=3$). Inset: SWV response for graphene nanoribbon– CoFe_2O_4 @NiO/HMIM PF_6 /CPE at different concentrations of Azi (10 μM to 2 mM) in PBS (pH 7.0)

Determination of Azi in real samples

Graphene nanoribbon– CoFe_2O_4 @NiO/HMIM PF_6 /CPE as an electrochemical sensor was checked by square wave voltammetry technique to determine Azi in the urine and Azi capsule as two real samples. The results with the acceptable recoveries are shown in Table 2.

Conclusion

In the present work, the Azi antibiotic was determined with a carbon paste electrode modified by nanomaterial and ion liquid. The electrocatalytic activity of the proposed Azi sensor was improved by nanoribbon– CoFe_2O_4 @NiO nanocomposite and 1-hexyl-3-methylimidazolium hexafluorophosphate as an ionic liquid. The pH study was carried out in different ranges of PBS in presence of Azi and the results revealed that the fabricated sensor has the best performance in pH 7.0. Also, the results demonstrated the number of

Table 2 Analytical applicability of suggested electrode in Azi capsule and urine samples

Sample	Azi added (μM)	Azi founded (μM)	Recovery (%)
Capsule	–	5.50 ± 1.72	–
Capsule	80.00	81.45 ± 0.35	95.26
Capsule	100.00	102.51 ± 2.22	97.16
Urine	–	2.47 ± 0.17	–
Urine	60.00	60.19 ± 0.84	96.35
Urine	80.00	81.84 ± 1.24	99.23

electrons and protons in the reaction is the same. Moreover, the scan rate investigation showed that Azi electro-oxidation is diffusion controlled and the diffusion coefficient value ($D=9.22 \times 10^{-6} \text{ cm}^2/\text{s}$) was calculated by chronoamperometry study. Furthermore, the wide linear ranges from 10 μM to 2 mM with a LOD of 0.66 μM were obtained. In addition, the low signal fluctuations are approved for good stability of the resultant sensor. As well as, the reproducibility (RSD ~ 3.15%), repeatability (RSD ~ 2.5%), and selectivity tests were performed, which all were acceptable. Eventually, the applicability of the fabricated Azi sensor was assessed by testing in the urine sample and the Azi capsule as real samples. Consequently, the acceptable recovery percentages for the urine sample (95.26–97.16%) and the Azi capsule (96.35–99.23%) confirmed the applicability of the proposed sensor.

Table 1 Comparison with some recently reported electrochemical sensors of Azi

Electrode	Mediator	Linear range (μM)	Limit of detection (μM)	References
CPE	Au nanoparticles	0.2–3.12	0.06	Vajdle et al. (2020)
GCE	Gr/IL	0.65–38.25	0.25	Peng et al. (2011)
GCE	MgCr_2O_4 /MWCNT	0.25–10.0	0.07	Ensafi et al. (2013)
Coated graphite	Azi-imprinted polymers	2–10,000	0.7	Abu-Dalo et al. (2015)
CPE	Graphene nanoribbon– CoFe_2O_4 @NiO/HMIM PF_6	10–2000	0.66	This work

Acknowledgements We thank the research councils of the Iran University of Science and Technology for supporting this project.

Data availability All data generated or analysed during this study are included in this published article (and its supplementary information file).

References

- Abdi R et al (2020) Determining caffeic acid in food samples using a voltammetric sensor amplified by Fe₃O₄ nanoparticles and room temperature ionic liquid. *Int J Electrochem Sci* 15:2539–2548
- Abedini S, Rafati AA, Ghaffarinejad A (2022) A simple and low-cost electrochemical sensor based on a graphite sheet electrode modified by carboxylated multiwalled carbon nanotubes and gold nanoparticles for detection of acyclovir. *New J Chem* 46(42):20403–20411
- Abu-Dalo MA et al (2015) Azithromycin-molecularly imprinted polymer based on PVC membrane for azithromycin determination in drugs using coated graphite electrode. *J Electroanal Chem* 751:75–79
- Alreja G et al (2012) Rhabdomyolysis caused by an unusual interaction between azithromycin and simvastatin. *J Cardiovasc Dis Res* 3(4):319–322
- Ashrafzadeh Afshar E et al (2022) Magnetic nanoparticles based on cerium MOF supported on the MWCNT as a fluorescence quenching sensor for determination of 6-mercaptopurine. *Environ Pollut* 305:119230
- Baladi E, Davar F, Hojjati-Najafabadi A (2022) Synthesis and characterization of g-C₃N₄-CoFe₂O₄-ZnO magnetic nanocomposites for enhancing photocatalytic activity with visible light for degradation of penicillin G antibiotic. *Environ Res* 215:114270
- Bijad M et al (2018) An electrochemical-amplified-platform based on the nanostructure voltammetric sensor for the determination of carmoisine in the presence of tartrazine in dried fruit and soft drink samples. *J Food Meas Charact* 12(1):634–640
- Bijad M et al (2021) An overview of modified sensors with focus on electrochemical sensing of sulfite in food samples. *Eurasian Chem Commun* 3(2):116–138
- Breier A et al (2002) Microbiological assay for azithromycin in pharmaceutical formulations. *J Pharm Biomed Anal* 29(5):957–961
- Buledi JJA et al (2022) Fabrication of sensor based on polyvinyl alcohol functionalized tungsten oxide/reduced graphene oxide nanocomposite for electrochemical monitoring of 4-aminophenol. *Environ Res* 212:113372
- Champney WS, Burdine R (1995) Macrolide antibiotics inhibit 50S ribosomal subunit assembly in *Bacillus subtilis* and *Staphylococcus aureus*. *Antimicrob Agents Chemother* 39(9):2141–2144
- Choemunng A, Na-Bangchang K (2010) An alternative liquid chromatography-mass spectrometric method for the determination of azithromycin in human plasma and its application to pharmacokinetic study. *J Liq Chromatogr Relat Technol* 33(16):1516–1528
- Chorin E et al (2020) The QT interval in patients with COVID-19 treated with hydroxychloroquine and azithromycin. *Nat Med* 26(6):808–809
- Coguplugil ZK et al (2022) Synthesis and characterization of Pt/ZnO@SWCNT/Fe₃O₄ as a powerful catalyst for anodic part of direct methanol fuel cell reaction. *Int J Hydrogen Energy*. <https://doi.org/10.1016/j.ijhydene.2022.10.238>
- Ensafi AA, Karimi-Maleh H (2010) Modified multiwall carbon nanotubes paste electrode as a sensor for simultaneous determination of 6-thioguanine and folic acid using ferrocene dicarboxylic acid as a mediator. *J Electroanal Chem* 640(1–2):75–83
- Ensafi AA, Karimi-Maleh H, Mallakpour S (2011a) N-(3,4-Dihydroxyphenethyl)-3, 5-dinitrobenzamide-modified multiwall carbon nanotubes paste electrode as a novel sensor for simultaneous determination of penicillamine, uric acid, and tryptophan. *Electroanalysis* 23(6):1478–1487
- Ensafi AA et al (2011b) Characterization of Mn-nanoparticles decorated organo-functionalized SiO₂-Al₂O₃ mixed-oxide as a novel electrochemical sensor: application for the voltammetric determination of captopril. *J Mater Chem* 21(38):15022–15030
- Ensafi AA, Allafchian AR, Rezaei B (2013) A sensitive and selective voltammetric sensor based on multiwall carbon nanotubes decorated with MgCr₂O₄ for the determination of azithromycin. *Colloids Surf B* 103:468–474
- Farghaly OAE-M, Mohamed NAL (2004) Voltammetric determination of azithromycin at the carbon paste electrode. *Talanta* 62(3):531–538
- Filist M et al (2014) Simplified LC-MS/MS method enabling the determination of azithromycin in human plasma after a low 100 mg dose administration. *J Pharm Biomed Anal* 100:184–189
- Gautret P et al (2021) Hydroxychloroquine and azithromycin as a treatment of COVID-19: results of an open label non-randomized clinical trial revisited. *Int J Antimicrob Agents* 57(1):106243
- Ghaffarinejad A et al (2014) A simple method for determination of D-penicillamine on the carbon paste electrode using cupric ions. *Bioelectrochemistry* 99:53–56
- Gielen V, Johnston SL, Edwards MR (2010) Azithromycin induces anti-viral responses in bronchial epithelial cells. *Eur Respir J* 36(3):646–654
- Grimshaw J (2000) Electrochemical reactions and mechanisms in organic chemistry. Elsevier, New York
- Hashemi M et al (2022) Pre-deposited alkali (Li, Na, K) chlorides layer for effective doping of CuInS₂ thin films as absorber layer in solar cells. *Sol Energy* 231:694–704
- Heidari M, Ghaffarinejad A (2019) Electrochemical sensor for L-cysteine by using a cobalt(II)/aluminum(III) layered double hydroxide as a nanocatalyst. *Microchim Acta* 186(6):365
- Hojjati-Najafabadi A et al (2021) Antibacterial and photocatalytic behaviour of green synthesis of Zn_{0.95}Ag_{0.05}O nanoparticles using herbal medicine extract. *Ceram Int* 47(22):31617–31624
- Hojjati-Najafabadi A et al (2022a) A review on magnetic sensors for monitoring of hazardous pollutants in water resources. *Sci Total Environ* 824:153844
- Hojjati-Najafabadi A et al (2022b) A tramadol drug electrochemical sensor amplified by biosynthesized au nanoparticle using mentha aquatic extract and ionic liquid. *Top Catal* 65(5):587–594
- Hojjati-Najafabadi A et al (2022c) Magnetic-MXene-based nanocomposites for water and wastewater treatment: a review. *J Water Process Eng* 47:102696
- Hu L et al (2018) A rapid and sensitive molecularly imprinted electrochemiluminescence sensor for azithromycin determination in biological samples. *J Electroanal Chem* 813:1–8
- Jafarzadeh H et al (2022) Hydrogen production via sodium borohydride hydrolysis catalyzed by cobalt ferrite anchored nitrogen-and sulfur co-doped graphene hybrid nanocatalyst: artificial neural network modeling approach. *Chem Eng Res Des* 183:557–566
- Jahani PM et al (2020) Application of TiO₂/Fe₃O₄/MWCNTs nanocomposite conductive mediator for fabrication of kojic acid sensor. *Int J Electrochem Sci* 15:5712–5722
- Jayanna B, Nagendrappa G, Gowda N (2012) Spectrophotometric estimation of azithromycin in tablets. *Indian J Pharm Sci* 74(4):365
- Karaman C et al (2022) Congo red dye removal from aqueous environment by cationic surfactant modified-biomass derived carbon: equilibrium, kinetic, and thermodynamic modeling, and

- forecasting via artificial neural network approach. *Chemosphere* 290:133346
- Karimi F et al (2022) An applicable method for extraction of whole seeds protein and its determination through Bradford's method. *Food Chem Toxicol* 164:113053
- Karimi-Maleh H, Ensafi A, Allafchian A (2010) Fast and sensitive determination of captopril by voltammetric method using ferrocenedicarboxylic acid modified carbon paste electrode. *J Solid State Electrochem* 14(1):9–15
- Karimi-Maleh H et al (2013) A voltammetric sensor based on NiO nanoparticle-modified carbon-paste electrode for determination of cysteamine in the presence of high concentration of tryptophan. *J Chem* 2013:7. <https://doi.org/10.1155/2013/946230>
- Karimi-Maleh H et al (2022a) A green and sensitive guanine-based DNA biosensor for idarubicin anticancer monitoring in biological samples: a simple and fast strategy for control of health quality in chemotherapy procedure confirmed by docking investigation. *Chemosphere* 291:132928
- Karimi-Maleh H et al (2022b) Cyanazine herbicide monitoring as a hazardous substance by a DNA nanostructure biosensor. *J Hazard Mater* 423:127058
- Karimi-Maleh H et al (2022c) Determination of D&C Red 33 and Patent Blue V Azo dyes using an impressive electrochemical sensor based on carbon paste electrode modified with ZIF-8/g-C₃N₄/Co and ionic liquid in mouthwash and toothpaste as real samples. *Food Chem Toxicol* 162:112907
- Karimi-Maleh H et al (2022d) Recent advances in carbon nanomaterials-based electrochemical sensors for food azo dyes detection. *Food Chem Toxicol* 164:112961
- Khatoun A et al (2022) A fast and reliable electrophoretic method for size-based characterization of silver nanoparticles. *Ind Eng Chem Res*
- Maaz K et al (2007) Synthesis and magnetic properties of cobalt ferrite (CoFe₂O₄) nanoparticles prepared by wet chemical route. *J Magn Magn Mater* 308(2):289–295
- Mahmoudi E, Behnajady MA (2018) Synthesis of Fe₃O₄@NiO core-shell nanocomposite by the precipitation method and investigation of Cr(VI) adsorption efficiency. *Colloids Surf A* 538:287–296
- Mandić Z, Weitner Z, Ilijaš M (2003) Electrochemical oxidation of azithromycin and its derivatives. *J Pharm Biomed Anal* 33(4):647–654
- Mansoorianfar M et al (2022) Recent progress on adsorption of cadmium ions from water systems using metal-organic frameworks (MOFs) as an efficient class of porous materials. *Environ Res* 214:114113
- Mater Mahnashi H et al (2021) Simultaneous electrochemical detection of azithromycin and hydroxychloroquine based on VS₂ QDs embedded N, S @graphene aerogel/cCNTs 3D nanostructure. *Microchem J* 163:105925
- Montenez J-P et al (1996) Interaction of the macrolide azithromycin with phospholipids. II. Biophysical and computer-aided conformational studies. *Eur J Pharmacol* 314(1–2):215–227
- Mostafazadeh R, Ghaffarinejad A, Tajabadi F (2022) A caffeic acid electrochemical sensor amplified with GNR/CoFe₂O₄@NiO and 1-ethyl-3-methylimidazolium acetate; a new perspective for food analysis. *Food Chem Toxicol* 167:113312
- Motaghi MM et al (2016) Nanostructure electrochemical sensor for voltammetric determination of vitamin C in the presence of vitamin B6: application to real sample analysis. *Int J Electrochem Sci* 11(9):7849
- Nigović B (2004) Adsorptive stripping voltammetric determination of azithromycin at a glassy carbon electrode modified by electrochemical oxidation. *Anal Sci* 20(4):639–643
- Parnham MJ et al (2014) Azithromycin: mechanisms of action and their relevance for clinical applications. *Pharmacol Ther* 143(2):225–245
- Peng JY et al (2011) Electrochemical behavior of azithromycin at graphene and ionic liquid composite film modified electrode. *Talanta* 86:227–232
- Rachidi M et al (2006) New spectrophotometric method for azithromycin determination. *Anal Lett* 39(9):1917–1926
- Rao L et al (2022) Lotus seedpods biochar decorated molybdenum disulfide for portable, flexible, outdoor and inexpensive sensing of hyperin. *Chemosphere* 301:134595
- Scherrer P (1912) Bestimmung der inneren Struktur und der Größe von Kolloidteilchen mittels Röntgenstrahlen. In: *Kolloidchemie Ein Lehrbuch*. Springer, pp 387–409
- Shamsadin-Azad Z et al (2019) A nanostructure voltammetric platform amplified with ionic liquid for determination of tert-butylhydroxyanisole in the presence kojic acid. *J Food Meas Charact* 13(3):1781–1787
- Sharma TSK, Hwa K-Y (2022) Architecting hierarchal Zn₃V₂O₈/P-rGO nanostructure: electrochemical determination of anti-viral drug azithromycin in biological samples using SPCE. *Chem Eng J* 439:135591
- Shawabkeh RA, Tutunji MF (2002) Mathematical modelling of the electrode process of azithromycin using cyclic voltammetry at hanging mercury drop electrode. *Sensors* 2(11):436–446
- Shepard R et al (1991) High-performance liquid chromatographic assay with electrochemical detection for azithromycin in serum and tissues. *J Chromatogr B Biomed Sci Appl* 565(1–2):321–337
- Sultana J et al (2020) Azithromycin in COVID-19 patients: pharmacological mechanism, clinical evidence and prescribing guidelines. *Drug Saf* 43(8):691–698
- Tajik S, Taher MA, Beitollahi H (2014) The first electrochemical sensor for determination of mangiferin based on an ionic liquid-graphene nanosheets paste electrode. *Ionics* 20(8):1155–1161
- Torkian N et al (2022) Synthesis and characterization of Ag-ion-exchanged zeolite/TiO₂ nanocomposites for antibacterial applications and photocatalytic degradation of antibiotics. *Environ Res* 207:112157
- Vajdle O et al (2020) Use of carbon paste electrode and modified by gold nanoparticles for selected macrolide antibiotics determination as standard and in pharmaceutical preparations. *J Electroanal Chem* 873:114324
- Wang H et al (2000) Adsorptive stripping voltammetric determination of erythromycin at a pretreated glassy carbon electrode. *Microchem J* 64:67–71
- Zeng A et al (2014) Determination of azithromycin in raw materials and pharmaceutical formulations by HPLC coupled with an evaporative light scattering detector. *Asian J Pharm Sci* 9(2):107–116
- Zheng Y, Karimi-Maleh H, Fu L (2022) Evaluation of antioxidants using electrochemical sensors: a bibliometric analysis. *Sensors* 22(9):3238
- Zhou T et al (2016) Fabrication of a selective and sensitive sensor based on molecularly imprinted polymer/acetylene black for the determination of azithromycin in pharmaceuticals and biological samples. *PLoS One* 11(1):e0147002

Publisher's Note Springer Nature remains neutral with regard to jurisdictional claims in published maps and institutional affiliations.

Springer Nature or its licensor (e.g. a society or other partner) holds exclusive rights to this article under a publishing agreement with the author(s) or other rightsholder(s); author self-archiving of the accepted manuscript version of this article is solely governed by the terms of such publishing agreement and applicable law.